

Quantum speed-up in collisional battery charging

Stella Seah,^{1,*} Martí Perarnau-Llobet,¹ Géraldine Haack,¹ Nicolas Brunner,¹ and Stefan Nimmrichter^{2,†}

¹Département de Physique Appliquée, Université de Genève, 1211 Genève, Switzerland

²Naturwissenschaftlich-Technische Fakultät, Universität Siegen, Siegen 57068, Germany

(Dated: July 25, 2022)

We present a collision model to describe the charging of a quantum battery by identical non-equilibrium qubit units. When the units are prepared in a classical mixture of energy eigenstates, the energy gain in the battery can be described by a classical random walk, so that both average energy and variance grow linearly with time. In contrast, when the qubits feature quantum coherence, we show that interference effects build up in the distribution of the battery, leading to a fast spreading of its energy variance (quadratic in time), reminiscent of a quantum random walk. By initializing the battery in the ground state, such interference effects can be exploited for faster and more efficient battery charging. In particular, we show that coherent protocols can lead to higher charging power than any possible incoherent strategy. This demonstrates a quantum speed-up at the level of a single battery. Finally, we characterise the amount of extractable work from the battery through the notion of ergotropy.

The development of thermodynamic protocols that exploit quantum effects such as coherences and entanglement to outperform their classical counterparts has been a major focus in the field of quantum thermodynamics [1, 2]. A simple scenario to explore this question is a *quantum battery*: a quantum system that can receive or supply energy [3–5]. Examples range from simple qubit batteries [6, 7], collective spins [8], interacting spin chains [9, 10], to mechanical flywheels [11–13].

In a seminal work, Alicki and Fannes developed the first quantum advantage in these devices: given a set of independent batteries, entangling operations allow for extracting more work than local ones [3]. Recently afterwards, the relevance of entanglement for power of battery charging was characterised in [7, 14, 15]. In parallel, several implementations for quantum batteries were proposed in cavity and waveguide QED setups, where the quantum advantage arises due to a collective superradiant coupling [16–20], while speed-ups driven by many-body interactions were explored in [9, 21–24]. Theoretical bounds for such collective advantages have been derived in [10]. Motivated by these developments, charging processes that exploit (or suffer from) dissipation [25–29], stabilisation mechanisms [30–34], and the impact of non-negligible energy fluctuations [35–40] have also been investigated.

In this work, we explore a different kind of quantum advantage in battery charging, which takes place at the level of a single device and hence does not have a collective origin. Instead, it arises due to the quantum nature of the charging protocol. Any charging process involves an auxiliary system that is used to charge the battery; this may be a thermal engine [11, 41, 42], an external time-dependent field [4, 7, 15], a quantized light field [16–20], or more generally an out-of-equilibrium (quantum) system [8]. We are interested in comparing processes where the charging source has either a classical or quantum nature. For that, we model battery charging using a collision, or repeated interaction, model [42–46].

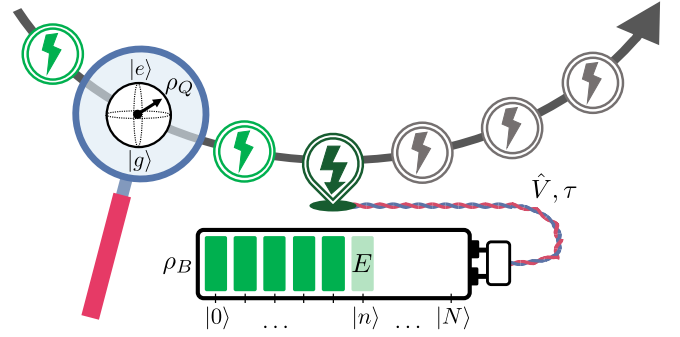


FIG. 1. Sketch of the collisional battery charging protocol. The battery is modeled as a uniform energy ladder with $N + 1$ levels in steps of E . Its quantum state ρ_B receives energy “charge” from a stream of identical qubits prepared in the state ρ_Q , via the resonant exchange interaction \hat{V} applied for a time τ .

Collision models have proven useful to, e.g., understand equilibration and non-equilibrium dynamics [43–45, 47, 48], the impact of quantum coherence in thermodynamics [49, 50], as well as strong coupling thermodynamics [51]; and here we explore its potential in the context of battery charging.

By describing the charging process as a collision model (see Fig. 1), we find that energy coherences in the charging units can generate interference effects in the battery. This leads to a fast spread of the battery’s energy distribution, whose variance increases quadratically in time (in contrast to the linear increase found for classical units). This fast-mixing behaviour is reminiscent of quantum random walks [52–54], which play a crucial role in speeding up quantum algorithms [55–57], and we develop similar advantages in quantum thermodynamics. In particular, we find that coherently prepared units can lead to higher charging than their classical counterparts when the battery starts in the ground state. Notably, when charging power becomes the figure of merit, quantum protocols can overcome arbitrary classical ones for a fixed energy rate between units and battery. Finally, we study the efficiency of these charging processes, by comparing the ergotropy [58] in the battery with that of the charging units.

* stella.seah@unige.ch

† stefan.nimmrichter@uni-siegen.de

Model.—We consider a quantum battery with Hamiltonian $\hat{H}_B = E \sum_0^N n |n\rangle \langle n|$ and lowering operator $\hat{A} = \sum_1^N |n-1\rangle \langle n|$ where $(N+1)$ denotes the number of levels in the battery [41, 59].

The battery shall be charged by sequential interactions using incoming *resonant* qubits with bare Hamiltonian $\hat{H}_Q = E |e\rangle \langle e|$ where $|g\rangle, |e\rangle$ denote the ground and excited qubit states.

We consider the swap interaction $\hat{V} = \hbar g(\hat{\sigma}_+ \hat{A} + \hat{\sigma}_- \hat{A}^\dagger)$ acting for a time τ at each charging step, which can be characterized by a single parameter $\theta = g\tau$. Since the unitary generated by \hat{V} is a thermal operation, i.e. $[\hat{V}, \hat{H}_B + \hat{H}_Q] = 0$ [60, 61], the coupling of the battery to the probes will not require external work [62].

Consider an arbitrary qubit state written as

$$\rho_Q = q |g\rangle \langle g| + (1-q) |e\rangle \langle e| + c \sqrt{q(1-q)} (e^{i\alpha} |e\rangle \langle g| + h.c.), \quad (1)$$

with $q \in [0, 1]$ the ground-state occupation, $\alpha \in [0, 2\pi]$ the phase, and $c \in [0, 1]$ the degree of coherence. The qubit contains an average energy $E(1-q)$, which can be partly transferred to the battery via \hat{V} .

The transformation of the battery state $\rho_B \rightarrow \rho'_B$ after one charge step can be expressed in terms of a Lindblad generator, $\Delta\rho_B = \rho'_B - \rho_B = \mathcal{L}\rho_B$. For a given parameter q , we distinguish the two opposing cases of incoherent charging ($c = 0$) via diagonal qubit states and coherent charging ($c = 1$) via pure superposition states.

In the rotating frame with respect to $\hat{H}_B + \hat{H}_Q$, we get generators

$$\begin{aligned} \mathcal{L}_{\text{inc}}\rho_B &= \sin^2 \theta (q \mathcal{D}[\hat{A}]\rho_B + (1-q) \mathcal{D}[\hat{A}^\dagger]\rho_B) \\ &+ (1 - \cos \theta)^2 (q \mathcal{D}[|0\rangle\langle 0|]\rho_B + (1-q) \mathcal{D}[|N\rangle\langle N|]\rho_B) \end{aligned} \quad (2)$$

for the incoherent case and

$$\begin{aligned} \mathcal{L}_{\text{coh}}\rho_B &= -i \sqrt{q(1-q)} \sin \theta \cos \theta [\hat{A} e^{-i\alpha} + \hat{A}^\dagger e^{i\alpha}, \rho_B] \\ &+ \mathcal{D}[\sqrt{q} \sin \theta \hat{A} + i e^{i\alpha} \sqrt{1-q} (1 - \cos \theta) |N\rangle\langle N|] \rho_B \\ &+ \mathcal{D}[\sqrt{1-q} \sin \theta \hat{A}^\dagger + i e^{-i\alpha} \sqrt{q} (1 - \cos \theta) |0\rangle\langle 0|] \rho_B \end{aligned} \quad (3)$$

for the coherent case, where $\mathcal{D}[\hat{B}]\rho = \hat{B}\rho\hat{B}^\dagger - \{\hat{B}^\dagger\hat{B}, \rho\}/2$. The general case of partially coherent qubits simply results in a mixture of the two generators, $\mathcal{L}\rho_B = c \mathcal{L}_{\text{coh}}\rho_B + (1-c) \mathcal{L}_{\text{inc}}\rho_B$.

For the incoherent generator \mathcal{L}_{inc} , the first line in (2) describes incoherent jumps up and down the energy ladder, conditioned on the qubit's ground-state and excitation probabilities q and $1-q$, respectively. This constitutes a random walk with the overall jump probability $p_\theta = \sin^2 \theta$ per step and leads to an average energy change per charge step of

$$\text{tr}\{\hat{H}_B \mathcal{L}_{\text{inc}}\rho_B\} = p_\theta(1-2q)E =: vE. \quad (4)$$

Naturally, average energy growth requires population inversion, $q < 1/2$. The parameter v denotes the (classical) dimensionless drift velocity across the ladder of battery levels per charge step. For a finite battery, the jumps are complemented

by a dephasing of the boundary states, as described in the second line. This is because, if no jump occurs, a ground-state (excited) qubit would learn that the battery is empty (full). The dephasing is of no relevance if the battery has no energy coherence to start with.

The coherent generator \mathcal{L}_{coh} (3) contains all the incoherent terms with additional cross-terms and an effective coherent driving Hamiltonian (first line). This driving term can generate interference effects in the case of strictly *partial* swaps ($\sin 2\theta \neq 0$). We shall identify the effective Rabi parameter

$$\Omega := 2 \sqrt{q(1-q)} \sin \theta \cos \theta = \sqrt{q(1-q)} \sin 2\theta, \quad (5)$$

which will quantify the coherent speedup of battery charging.

Incoherent charging.—Let us first consider the classical incoherent charging of the battery assuming an initially diagonal battery state in the eigenbasis of \hat{H}_B and diagonal charging qubits with $c = 0$. One can see from (2) that the battery state then remains diagonal, fully characterized by the populations $P(n, k) = \langle n | \rho_B(k) | n \rangle$ after interaction with the k -th qubit.

We first focus on the regime where the battery does not populate the boundary states $|0\rangle$ and $|N\rangle$, i.e., we omit the presence of boundaries. Then, we obtain a discrete random walk with three branches per time step, as described by the update rule

$$P(n, k+1) = (1-p_\theta)P(n, k) + p_\theta(1-q)P(n-1, k) + p_\theta q P(n+1, k), \quad (6)$$

valid for $0 < n < N$. The energy profile hence performs a random walk in which the number of jumps up/down or no jumps after k interactions, $\mathbf{X} = \{X_+, X_-, X_0\}$, follows a trinomial distribution with probabilities $\mathbf{p} = \{p_\theta q, p_\theta(1-q), 1-p_\theta\}$ [63]. The mean and variance of charge n (energy in units E) grow linearly in time,

$$\bar{n}(k) = \bar{n}(0) + vk, \quad \Delta n^2(k) = \Delta n^2(0) + (p_\theta - v^2)k, \quad (7)$$

with $\bar{n}(k) = \sum_n n P(n, k)$ and $\Delta n^2(k) = \sum_n n^2 P(n, k) - \bar{n}(k)^2$. Taking $k \gg 1$ (but still neglecting the boundaries), the trinomial distribution has two natural limits: For small jump probabilities ($p_\theta \ll 1$) and finite $k p_\theta$, the numbers of jumps up/down obey a Poisson distribution with mean $k p_\pm$ [64, 65]. Conversely, for large k and moderate $p_\theta \neq 0, 1$, the random variable \mathbf{X} follows a Gaussian distribution in accordance with the central limit theorem, refer to App. B. At the boundaries of zero and full charge, the energy distribution gets reflected and the battery eventually converges to a Gibbs state, $P(n, \infty) \propto (1-q)^n / q^n$, at the effective (negative) qubit temperature defined by $e^{-E/k_B T} = (1-q)/q$. *Coherent charging and quantum signatures.*—Now, instead of using classical population-inverted states to charge the battery, let us consider qubit states prepared in pure superposition state with the same occupation q . The coherent state has the same mean energy but a higher purity, which can be interpreted as a thermodynamic resource (see e.g. [49, 50]). Since \hat{V} is invariant under rotation about the z -axis, we set the qubit phase $\alpha = 0$ without loss of generality.

Far from the charge limits of the battery (i.e., neglecting the boundaries), we show in App. C that a bimodal energy distribution emerges, whose two branches simultaneously progress

down and up the energy ladder with increasing number of interactions k .

For an initially pure battery state $|n_0\rangle$ and sufficiently large k (with $n_0 - k > 0$ and $n_0 + k < N$), the two branches will be peaked approximately at the positions

$$n_{\pm} \approx n_0 + (v \pm c\Omega)k \quad (8)$$

on the energy ladder. The coherent driving thus speeds up one of the peaks by $c\Omega$ and slows down the other by the same amount, which results in the same mean energy increase as in the incoherent case (7). However, the energy variance now increases quadratically with k ,

$$\Delta n^2(k) \approx (p_\theta - v^2)k + \frac{c^2\Omega^2}{2}k(k-1). \quad (9)$$

The difference between classical and quantum charging is well captured by the Fano factor: $F \equiv \Delta n^2(k)/\bar{n}(k)$. For $k \gg 1$, classical processes give $F \approx (p_\theta - v^2)/v$, whereas $F \approx kc^2\Omega^2/2v$ for quantum ones. The growing F with k can be seen as a genuine quantum signature in this model.

Exemplary snapshots of the energy distribution of the battery are depicted in Fig. 2(a) for both coherent (red curves) and the respective incoherent counterpart (black curves) for increasing k . The incoherent charging processes are well described by Gaussians whose mean values (black dotted lines) move according to (7). The red-dotted lines mark the approximate peak positions for the coherent case according to (8), which agree well with the actual maxima of the distributions. Note also that the average energy $\bar{n}(k)$ is the same between incoherent and coherent case as long as the boundaries are not hit. When this happens, the evolutions drastically change: the quantum wave is reflected, whereas the classical distribution tends to the inverse Gibbs state.

Quantum advantage for empty batteries.—At first sight, the previous considerations suggest that quantum coherence is not beneficial for battery charging: coherent qubits provide at most the same average energy to the battery as incoherent ones, and with a larger variance. The situation drastically changes when considering the relevant situation where the battery starts in its ground state. In this case, the decaying branch in (8) is smeared out due to the presence of the boundary, while the other sharply peaked branch of the distribution plays the dominant role of increasing the battery's charge.

A significant quantum advantage can be observed if we consider charging an initially empty battery ($n_0 = 0$), with either classical ($c = 0$) or coherent ($c = 1$) qubits at the same average energy (q), see Fig. 2(b). We observe a suppression of the branch that decreases the energy, and a single forward-propagating peak. Even though our analytic random-walk model no longer applies, we find that the peak position is still situated close to the value n_+ from (8), which climbs up the ladder at a 73% faster rate than the incoherent Gaussian for $q = 0.25$. We compare the corresponding energy growth in Fig. 3(a); and in (b) for the more distinctive case $q = 0.49$. So long as the battery is far from the fully-charged state, coherent charging is always more advantageous. However, once the maximum charge is reached, we see a drop in energy due

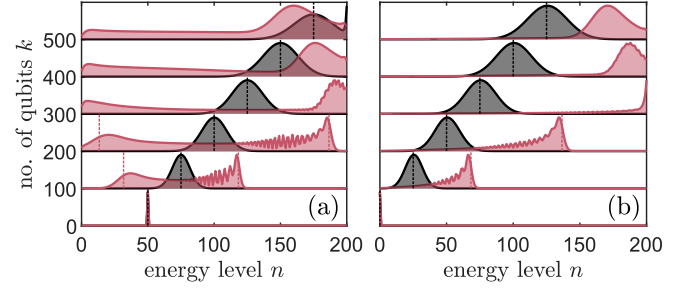


FIG. 2. Energy distributions of a battery of size $N = 200$ charged by k incoherent (black) and coherent (red) qubits with $q = 1/4$ and $\theta = \pi/4$. All curves are rescaled to the same maximum. In (a), the battery is initialized in the pure, partially charged state $|n_0 = 50\rangle$, whereas in (b), the battery is initialized in the zero-charge state $|0\rangle$. The dotted black and red vertical lines mark the approximate average charge according to (7) and the approximate peak positions (8) for incoherent and coherent qubits, respectively for $\bar{n} < 200$.

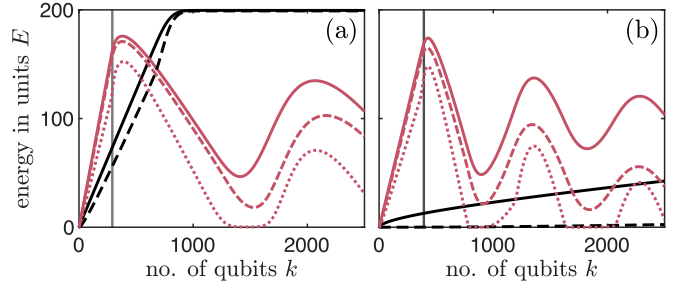


FIG. 3. Energy (solid) and ergotropy (dashed) for incoherent (black) and coherent (red) charging of a battery of $N = 200$ with k qubits. Here, (a) matches Fig. 2(b) with $q = 0.25$ and $n_0 = 0$ while (b) corresponds to $q = 0.49$. The dotted line shows the ergotropy associated to the dephased battery state, i.e. only the energy populations. The vertical lines mark the theoretical k_{est} in (10).

to reflection at the boundary $n = N$. The number of coherent steps from empty to maximum battery charge is therefore

$$k_{\text{est}} \approx \left\lfloor \frac{N}{c\Omega + v} \right\rfloor \quad (10)$$

For Fig. 3, this estimate amounts to (a) $k_{\text{est}} \approx 292$ and (b) 392, in good agreement with the depicted maxima.

The quantum advantage can be quantified by the ratio between the rate of energy charging between incoherent ($c = 0$) and coherent ($c = 1$) qubits:

$$\mathcal{A}(k) = \frac{\bar{n}_{c=1}(k) - \bar{n}_{c=1}(k-1)}{\bar{n}_{c=0}(k) - \bar{n}_{c=0}(k-1)} \quad (11)$$

Here the subindex c in $\bar{n}(k)$ distinguishes incoherent from coherent charging. There is a quantum advantage if $\mathcal{A} > 1$ for some k, q and θ . In the regime $N > k \gg 1$, we can obtain an upper bound on \mathcal{A} by noting that the increment of $\bar{n}_{c=1}$ is upper bounded by $v + \Omega$ (the rate of the fast-moving quantum peak), whereas the classical increment is, for the most part, given by v . That is,

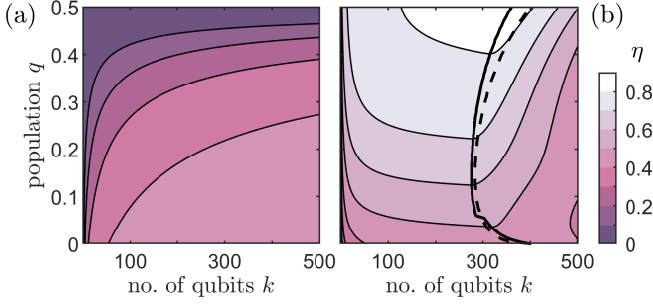


FIG. 4. (a) Incoherent and (b) coherent charging efficiency η for a battery of size $N = 200$ initialized in the zero-charge state for different k and q . Here, we consider $\theta = \pi/4$ where interference effects are the strongest. The solid line in (b) marks the number of qubits that maximises η for a given q -value, while the dashed line marks the estimate (10).

$$\mathcal{A} \lesssim 1 + \frac{\Omega}{\nu} = 1 + \frac{2\sqrt{q(1-q)}}{(1-2q)\tan\theta}. \quad (12)$$

It can be verified numerically that \mathcal{A} is always above 70% of this bound. Moreover, the quantum advantage diverges for $q \rightarrow 1/2$ and for $\theta \rightarrow 0$. Intuitively, this can be understood by noting that for $q \approx 1/2$, the incoherent charging vanishes whereas coherent charging is still possible.

On the other hand, for short interactions where $\theta \approx 0$, the quantum dynamics are governed by the coherent driving in (3), a process that is linear in θ , whereas classical charging takes place only at second order in θ .

Ergotropy and efficiency of the charging process.—Because energy fluctuations are inevitably present, in general not all average energy stored in the battery can be again reused as work. This effect is well captured by the notion of ergotropy [1, 58], which characterizes the amount of useful energy in the battery as the part that can be extracted by means of a deterministic unitary operation to bring it to a passive state [66, 67]. In Fig. 3, we plot the ergotropy together with the average energy of the battery.

When charged by coherent qubits, the battery stores ergotropy in two ways: by populating higher energies and by building up energy coherences. The proportion becomes apparent from the ergotropy that remains after dephasing the battery state in the energy basis (dotted curves in Fig. 3). We find that an initially empty battery stores most of the ergotropy in its energy profile until it reaches maximum charge. In the long time limit, however, ergotropy will approach a comparatively low steady-state value almost entirely stored in coherences.

For incoherent charging from the ground state, ergotropy grows monotonically until the battery converges to the inverted Gibbs state. One can then consider a hybrid charging protocol in which the battery is coherently charged until $k \approx k_{\text{est}}$ to exploit the quantum speedup, then incoherently charged up to the maximum charge if necessary.

Ergotropy also provides a natural way to define an efficiency of the charging process. The battery is charged by

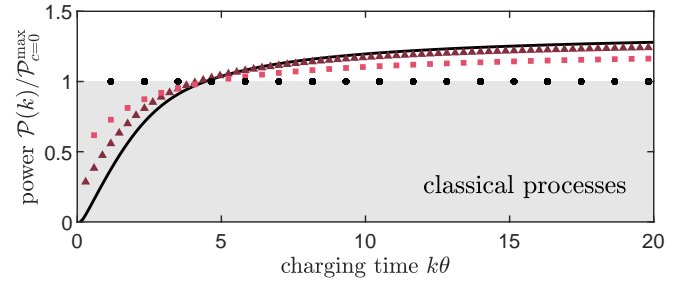


FIG. 5. Quantum advantage in terms of power normalized to the best incoherent charging protocol (circles), which uses a sequence of excited qubits ($q = 0$) with interaction parameter θ_{max} . The gray region thus bounds all classical processes. The solid curve represents the continuous quantum limit using $k \rightarrow \infty$ coherent qubits at $q = 1/2$. The squares and triangles represent coherent protocols for finite sequences of qubits with $q = 0.26$ and 0.38 interacting over $\theta = \theta_{\text{max}}/2$ and $\theta_{\text{max}}/4$, respectively. The chosen q -values are optimal in terms of power in the regime of $N > k \gg 1$.

qubits containing a finite amount of ergotropy \mathcal{E}_Q . We introduce the charging efficiency as the ratio of stored ergotropy over total ergotropy input after k steps, $\eta(k) = \mathcal{E}_B(k)/k\mathcal{E}_Q$. For energy-preserving interactions between units and battery, $\eta(k) \leq 1$ [37]. Figure 4 shows the efficiency for (a) the incoherent and (b) the coherent case as a function of k and q .

Coherent ergotropy transfer can reach more than 80% maximum efficiency at intermediate qubit numbers k , as indicated by the solid curve in Fig. 4(b) and compared against (10) (dashed). The efficiency drops again for greater k -values, as the battery's energy distribution hits the full-charge state $|N\rangle$ and then broadens in the adverse direction. Incoherent probes would continue to charge the battery to an inverted Gibbs state.

Quantum advantage in power.—The previous considerations show that quantum coherence can be exploited to enhance battery charging and its efficiency given a set of k qubits, each of them with average energy $(1-q)E$ and a fixed qubit-battery interaction θ . On the other hand, for a given k and θ , the energy charged into the battery, $\bar{n}(k)E$, is maximised for $q \rightarrow 0$. In this limit, the qubits are pure with perfect population inversion, so that the charging efficiency also increases, reaching $\eta(k) = 1$ in the case of full swaps. Crucially, this best-case-scenario ($q = 0$, $\theta = \pi/2$) makes no use of quantum coherence, and can be described as a classical stochastic process. This raises the natural question: can we find a quantum advantage against arbitrary classical protocols? Remarkably, this question can be answered affirmatively when power is the figure of merit and charging time is the only constraint.

Starting with an empty battery ($\bar{n}(0) = 0$), the average charging power of k qubits is $\mathcal{P}(k) = gE\bar{n}(k)/k\theta = E\bar{n}(k)/t$. It quantifies how much average energy the battery has gained over the charging time $t = k\theta/g$. The question we address is how to maximise \mathcal{P} over k and q at fixed t . For incoherent probes ($c = 0$), the power decreases monotonically with q , and the optimal classical strategy is hence obtained for $q = 0$, as expected. A straightforward calculation yields the fundamental upper bound for incoherent charging, $\mathcal{P}_{c=0}^{\text{max}} \approx 0.62gE$

attained at $\theta_{\max} \approx 1.17$.

Coherent probes can overcome this bound, as shown in Fig. 5. The optimal strategy consists in taking $q = 1/2$ and the limit of $\theta \rightarrow 0$ and $k \rightarrow \infty$, which caps the velocity of the fast-moving peak in (8) at $\Omega k/t \rightarrow g$ (solid line). In this case, the power is initially smaller, but after a transient buildup of quantum coherence in the battery, it quickly overcomes the incoherent bound (circles) until it reaches $\mathcal{P}_{c=1}^{\max} \approx 0.85gE = 1.37\mathcal{P}_{c=0}^{\max}$ at $1 \ll k < N$. In practice, one can achieve a significant coherent power enhancement already with a finite number of qubits (triangles and squares). Importantly, the advantage remains in terms of ergotropy. This is apparent in the limit $q = 1/2$ and $\theta \ll 1$, where the ergotropy matches exactly the increase in energy since the battery evolves unitarily up to first order in θ .

Conclusions.—We proposed a collision model for quantum battery charging, in which a set of identical qubits (the charging units) transfer energy to a finite energy ladder (the battery). We compared classical to quantum charging protocols,

in which the units are prepared in a mixture or superposition state, respectively. We found that quantum protocols can yield a higher power than arbitrary classical strategies, thus providing a clear advantage at the level of a single battery. This is complementary to previous examples of collective quantum speed-ups [4, 5].

Our analysis also highlights a connection between quantum thermodynamics and quantum random walks [52–54]. The formalism behind is however different: whereas in quantum random walks a single coin becomes entangled with the walker, here interference effects in the walker (i.e. the battery) are created through partial collision processes with a large number of coins (units). Future work could shed more light on the connection between both frameworks and exploit quantum walk-like features in thermodynamic protocols.

Acknowledgements.—M. P.-L. and G.H. acknowledge funding from Swiss National Science Foundation through an Ambizione grant PZ00P2-186067 and a starting grant PRIMA PR00P2-179748 respectively.

-
- [1] J. Goold, M. Huber, A. Riera, L. del Rio, and P. Skrzypczyk, *J. Phys. A* **49**, 143001 (2016).
 - [2] S. Vinjanampathy and J. Anders, *Contemp. Phys.* **57**, 545 (2016).
 - [3] R. Alicki and M. Fannes, *Phys. Rev. E* **87**, 042123 (2013).
 - [4] F. Campaioli, F. A. Pollock, and S. Vinjanampathy, in *Fundamental Theories of Physics* (Springer International Publishing, 2018) pp. 207–225.
 - [5] S. Bhattacharjee and A. Dutta, arXiv preprint arXiv:2008.07889 (2020).
 - [6] M. Horodecki and J. Oppenheim, *Nat. Commun.* **4**, 2059 (2013).
 - [7] F. C. Binder, S. Vinjanampathy, K. Modi, and J. Goold, *New J. Phys.* **17**, 075015 (2015).
 - [8] G. M. Andolina, M. Keck, A. Mari, V. Giovannetti, and M. Polini, *Phys. Rev. B* **99**, 205437 (2019).
 - [9] T. P. Le, J. Levinsen, K. Modi, M. M. Parish, and F. A. Pollock, *Phys. Rev. A* **97**, 022106 (2018).
 - [10] S. Julià-Farré, T. Salamon, A. Riera, M. N. Bera, and M. Lewenstein, *Phys. Rev. Research* **2**, 023113 (2020).
 - [11] A. Levy, L. Diósi, and R. Kosloff, *Phys. Rev. A* **93**, 052119 (2016).
 - [12] A. Roulet, S. Nimmrichter, J. M. Arrazola, S. Seah, and V. Scarani, *Phys. Rev. E* **95**, 062131 (2017).
 - [13] S. Seah, S. Nimmrichter, and V. Scarani, *New J. Phys.* **20**, 043045 (2018).
 - [14] K. V. Hovhannisyanyan, M. Perarnau-Llobet, M. Huber, and A. Acín, *Phys. Rev. Lett.* **111**, 240401 (2013).
 - [15] F. Campaioli, F. A. Pollock, F. C. Binder, L. Céleri, J. Goold, S. Vinjanampathy, and K. Modi, *Phys. Rev. Lett.* **118**, 150601 (2017).
 - [16] D. Ferraro, M. Campisi, G. M. Andolina, V. Pellegrini, and M. Polini, *Phys. Rev. Lett.* **120**, 117702 (2018).
 - [17] D. Ferraro, G. M. Andolina, M. Campisi, V. Pellegrini, and M. Polini, *Phys. Rev. B* **100**, 075433 (2019).
 - [18] G. M. Andolina, M. Keck, A. Mari, M. Campisi, V. Giovannetti, and M. Polini, *Phys. Rev. Lett.* **122**, 047702 (2019).
 - [19] F. Pirmoradian and K. Mølmer, *Phys. Rev. A* **100**, 043833 (2019).
 - [20] J. Monsel, M. Fellous-Asiani, B. Huard, and A. Auffèves, *Phys. Rev. Lett.* **124**, 130601 (2020).
 - [21] D. Rossini, G. M. Andolina, and M. Polini, *Phys. Rev. B* **100**, 115142 (2019).
 - [22] D. Rossini, G. M. Andolina, D. Rosa, M. Carrega, and M. Polini, *Phys. Rev. Lett.* **125**, 236402 (2020).
 - [23] D. Rosa, D. Rossini, G. M. Andolina, M. Polini, and M. Carrega, *J. High Energy Phys.* **2020**, 67 (2020).
 - [24] S. Ghosh, T. Chanda, and A. Sen(De), *Phys. Rev. A* **101**, 032115 (2020).
 - [25] F. Barra, *Phys. Rev. Lett.* **122**, 210601 (2019).
 - [26] D. Farina, G. M. Andolina, A. Mari, M. Polini, and V. Giovannetti, *Phys. Rev. B* **99**, 035421 (2019).
 - [27] F. H. Kamin, F. T. Tabesh, S. Salimi, F. Kheirandish, and A. C. Santos, *New J. Phys.* **22**, 083007 (2020).
 - [28] K. V. Hovhannisyanyan, F. Barra, and A. Imparato, *Phys. Rev. Research* **2**, 033413 (2020).
 - [29] F. T. Tabesh, F. H. Kamin, and S. Salimi, *Phys. Rev. A* **102**, 052223 (2020).
 - [30] A. C. Santos, B. Çakmak, S. Campbell, and N. T. Zinner, *Phys. Rev. E* **100**, 032107 (2019).
 - [31] S. Gherardini, F. Campaioli, F. Caruso, and F. C. Binder, *Phys. Rev. Research* **2**, 013095 (2020).
 - [32] J. Q. Quach and W. J. Munro, *Phys. Rev. Applied* **14**, 024092 (2020).
 - [33] A. C. Santos, A. Saguia, and M. S. Sarandy, *Phys. Rev. E* **101**, 062114 (2020).
 - [34] M. T. Mitchison, J. Goold, and J. Prior, arXiv:2012.00350 (2020).
 - [35] N. Friis and M. Huber, *Quantum* **2**, 61 (2018).
 - [36] E. McKay, N. A. Rodríguez-Briones, and E. Martín-Martínez, *Phys. Rev. E* **98**, 032132 (2018).
 - [37] M. Perarnau-Llobet and R. Uzdin, *New J. Phys.* **21**, 083023 (2019).
 - [38] L. P. García-Pintos, A. Hamma, and A. del Campo, *Phys. Rev. Lett.* **125**, 040601 (2020).
 - [39] A. Crescente, M. Carrega, M. Sassetti, and D. Ferraro, *New J. Phys.* **22**, 063057 (2020).
 - [40] F. Caravelli, G. Coulter-De Wit, L. P. García-Pintos, and

- A. Hamma, *Phys. Rev. Research* **2**, 023095 (2020).
- [41] N. Brunner, N. Linden, S. Popescu, and P. Skrzypczyk, *Phys. Rev. E* **85**, 051117 (2012).
- [42] E. Bäumer, M. Perarnau-Llobet, P. Kammerlander, H. Wilming, and R. Renner, *Quantum* **3**, 153 (2019).
- [43] V. Scarani, M. Ziman, P. Štelmachovič, N. Gisin, and V. Bužek, *Phys. Rev. Lett.* **88**, 97905 (2002).
- [44] L. Bruneau, A. Joye, and M. Merkli, *J. Math. Phys.* **55**, 75204 (2014).
- [45] D. Grimmer, D. Layden, R. B. Mann, and E. Martín-Martínez, *Phys. Rev. A* **94**, 032126 (2016).
- [46] P. Strasberg, G. Schaller, T. Brandes, and M. Esposito, *Phys. Rev. X* **7**, 021003 (2017).
- [47] S. Seah, S. Nimmrichter, and V. Scarani, *Phys. Rev. E* **99**, 042103 (2019).
- [48] M. Cattaneo, G. De Chiara, S. Maniscalco, R. Zambrini, and G. L. Giorgi, *Phys. Rev. Lett.* **126**, 130403 (2021).
- [49] F. L. S. Rodrigues, G. De Chiara, M. Paternostro, and G. T. Landi, *Phys. Rev. Lett.* **123**, 140601 (2019).
- [50] K. Hammam, Y. Hassouni, R. Fazio, and G. Manzano, *New J. Phys.* **23**, 043024 (2021).
- [51] P. Strasberg, *Phys. Rev. Lett.* **123**, 180604 (2019).
- [52] A. Ambainis, E. Bach, A. Nayak, A. Vishwanath, and J. Watrous, in *Proceedings of the Thirty-Third Annual ACM Symposium on Theory of Computing*, STOC '01 (Association for Computing Machinery, New York, NY, USA, 2001) p. 37–49.
- [53] J. Kempe, *Contemp. Phys.* **44**, 307 (2003).
- [54] E. Bach, S. Coppersmith, M. P. Goldschen, R. Joynt, and J. Watrous, *J. Comput. Syst. Sci.* **69**, 562 (2004).
- [55] A. M. Childs, R. Cleve, E. Deotto, E. Farhi, S. Gutmann, and D. A. Spielman, in *Proceedings of the Thirty-Fifth Annual ACM Symposium on Theory of Computing*, STOC '03 (Association for Computing Machinery, New York, NY, USA, 2003) p. 59–68.
- [56] V. M. Kendon, *Phil. Trans. R. Soc. A* **364**, 3407 (2006).
- [57] A. M. Childs, L. J. Schulman, and U. V. Vazirani, in *48th Annual IEEE Symposium on Foundations of Computer Science (FOCS'07)* (2007) pp. 395–404.
- [58] A. E. Allahverdyan, R. Balian, and T. M. Nieuwenhuizen, *Europhys. Lett.* **67**, 565 (2004).
- [59] P. Erker, M. T. Mitchison, R. Silva, M. P. Woods, N. Brunner, and M. Huber, *Phys. Rev. X* **7**, 031022 (2017).
- [60] F. Brandão, M. Horodecki, J. Oppenheim, J. M. Renes, and R. W. Spekkens, *Phys. Rev. Lett.* **111**, 250404 (2013).
- [61] F. Brandão, M. Horodecki, N. Ng, J. Oppenheim, and S. Wehner, *Proc. Natl. Acad. Sci.* **112**, 3275 (2015).
- [62] F. Barra, *Sci. Rep.* **5**, 14873 (2015).
- [63] J. Franke, W. K. Härdle, and C. M. Hafner, “Stochastic processes in discrete time,” in *Statistics of Financial Markets: An Introduction* (Springer Berlin Heidelberg, Berlin, Heidelberg, 2015) pp. 49–58.
- [64] G. F. Lawler and V. Limic, *Random Walk: A Modern Introduction*, Cambridge Studies in Advanced Mathematics (Cambridge University Press, 2010).
- [65] P. Deheuvels and D. Pfeifer, *J. Multivar. Anal.* **25**, 65 (1988).
- [66] W. Pusz and S. L. Woronowicz, *Commun. Math. Phys.* **58**, 273 (1978).
- [67] A. Lenard, *J. Stat. Phys.* **19**, 575 (1978).

Appendix A: Charging a quantum battery by a qubit

We model the quantum battery as a regular energy ladder of equidistant levels $|n\rangle$ separated by the energy gap E . It shall be charged in discrete steps of resonant energy exchange with identical qubits prepared in arbitrary quantum states ρ_Q , as mediated by the energy-preserving unitary

$$\hat{U}_\theta = \exp \left[-i\theta \left(\hat{A}|e\rangle\langle g| + \hat{A}^\dagger|g\rangle\langle e| \right) \right], \quad (\text{A1})$$

and its inverse $\hat{U}_\theta^\dagger = \hat{U}_{-\theta}$. Here, $|g\rangle, |e\rangle$ denote the qubit's ground and excited state and \hat{A}, \hat{A}^\dagger denote the lowering and raising operators on the battery ladder. The reduced battery state transforms as $\rho_B \rightarrow \rho'_B = \text{tr}_Q \{ \hat{U}_\theta \rho_B \otimes \rho_Q \hat{U}_{-\theta} \}$.

For an idealized, infinite battery, the ladder operators are defined through $\hat{A}|n\rangle = |n-1\rangle$ and $\hat{A}^\dagger|n\rangle = |n+1\rangle$ for all n , which leads to

$$\hat{U}_\theta|n, g\rangle = \cos \theta|n, g\rangle - i \sin \theta|n-1, e\rangle, \quad \hat{U}_\theta|n, e\rangle = \cos \theta|n, e\rangle - i \sin \theta|n+1, g\rangle. \quad (\text{A2})$$

Given a generic qubit state of the form

$$\rho_Q = q|g\rangle\langle g| + (1-q)|e\rangle\langle e| + c\sqrt{q(1-q)}\left(e^{-i\alpha}|g\rangle\langle e| + e^{i\alpha}|e\rangle\langle g|\right), \quad (\text{A3})$$

a straightforward application of (A2) shows that the transformation of the battery state after one step is

$$\begin{aligned} \langle n|\rho'_B|n'\rangle &= (1-p_\theta)\langle n|\rho_B|n'\rangle + p_\theta[(1-q)\langle n-1|\rho_B|n'-1\rangle + q\langle n+1|\rho_B|n'+1\rangle] \\ &\quad - ic\frac{\Omega}{2}\left[e^{i\alpha}(\langle n-1|\rho_B|n'\rangle - \langle n|\rho_B|n'+1\rangle) + e^{-i\alpha}(\langle n+1|\rho_B|n'\rangle - \langle n|\rho_B|n'-1\rangle)\right]. \end{aligned} \quad (\text{A4})$$

in the energy representation, with $p_\theta = \sin^2 \theta$ and $\Omega = \sqrt{q(1-q)} \sin 2\theta$. This transformation, which describes the time evolution of an infinite battery in discrete charging steps, can generate a classical or quantum random walk process depending on the chosen parameters θ, q, α, c . In the case of a finite battery with $N+1$ levels from the zero-charge state $|0\rangle$ to the fully charged $|N\rangle$, Eqs. (A2) and (A4) still hold for any $0 < n, n' < N$. Hence the infinite-battery results remain valid for those battery states that do not occupy $|0\rangle$ or $|N\rangle$.

In order to obtain an expression for the transformation of arbitrary finite-battery states, we can expand the unitary (A1) as

$$\hat{U}_\theta = \cos \theta \mathbb{1} - i \sin \theta \left(\hat{A} \otimes |e\rangle\langle g| + \hat{A}^\dagger \otimes |g\rangle\langle e| \right) + (1 - \cos \theta) (|0, g\rangle\langle 0, g| + |N, e\rangle\langle N, e|), \quad (\text{A5})$$

with $\hat{A} = \sum_{n=1}^N |n-1\rangle\langle n|$. Here, the last term accounts for the modified effect at the charge boundaries. Several steps of calculation reveal that the increment $\Delta\rho_B = \rho'_B - \rho_B = \mathcal{L}\rho_B$ can be expressed in terms of the Lindblad generator \mathcal{L} defined in the main text.

In the following, we study the time evolution of the battery state $\rho_B(k) = (\mathbb{1} + \mathcal{L})\rho_B(k-1) = (\mathbb{1} + \mathcal{L})^k \rho_B(0)$ after k charge steps, omitting boundary effects. We distinguish the opposite cases of incoherent charging ($c = 0$) and coherent charging ($c = 1$).

Appendix B: Incoherent battery charging

Assuming an initially diagonal battery state and diagonal qubits ($c = 0$), we are left with a classical discrete-time random walk model. The battery state remains diagonal at all times, and the populations transform according to a simple Markov chain with three branches: no jump with probability $1 - p_\theta$, jump up with $p_\theta(1 - q)$, jump down with $p_\theta q$. Denoting by $P(n, k) = \langle n|\rho_B(k)|n\rangle$ the populations of the battery at discrete time steps $k = 0, 1, \dots$, we get from (A4),

$$P(n, k+1) = (1 - p_\theta)P(n, k) + p_\theta(1 - q)P(n-1, k) + p_\theta q P(n+1, k). \quad (\text{B1})$$

This difference equation is *exact* for an infinite ladder as well as for a finite ladder at $0 < n < N$, which implies that its solution may serve as an approximation for transient states of finite ladders so long as the population at the charge boundaries is small. Specifically, the first and second moments and cumulants of charge n evolve as

$$\begin{aligned} \bar{n}(k) &= \sum_{n=-\infty}^{\infty} n P(n, k) = \bar{n}(k-1) + p_\theta(1 - 2q) = \bar{n}(0) + p_\theta(1 - 2q)k =: \bar{n}(0) + vk, \\ \overline{n^2}(k) &= \overline{n^2}(k-1) + p_\theta + 2p_\theta(1 - 2q)\bar{n}(k-1) = \overline{n^2}(k-1) + p_\theta + 2v\bar{n}(k-1), \\ \Delta n^2(k) &= \overline{n^2}(k) - \bar{n}^2(k) = \Delta n^2(k-1) + p_\theta - v^2 = \Delta n^2(0) + (p_\theta - v^2)k, \end{aligned} \quad (\text{B2})$$

indicating that the charge distribution spreads and drifts, as described by the stepwise increment $v = p_\theta(1 - 2q)$ of the mean charge. The time-evolved $P(n, k)$ can be expressed analytically in terms of the initial $P(n, 0)$ in various ways. For example, one can view the $P(n, k)$ as the n -th discrete Fourier coefficients of a periodic characteristic function $\chi(\phi, k) = \sum_n P(n, k)e^{in\phi}$ with $\phi \in (-\pi, \pi]$, normalized to $\chi(0, k) = 1$. The Markov chain (B1) translates into

$$\chi(\phi, k+1) = \left[(1 - p_\theta) + p_\theta(1 - q)e^{i\phi} + p_\theta q e^{-i\phi} \right] \chi(\phi, k) \Rightarrow \chi(\phi, k) = [1 - p_\theta(1 - \cos \phi) + iv \sin \phi]^k \chi(\phi, 0). \quad (\text{B3})$$

This amounts to a geometric progression by a factor of magnitude smaller than unity. Indeed, one can easily check that the magnitude of the square-bracketed expression is never greater than $\sqrt{1 - 4p_\theta(1 - p_\theta)\sin^2(\phi/2)}$ for any q . Hence, after sufficiently many time steps, the bracketed term will have suppressed the initial characteristic function almost everywhere except for a narrow region around $\phi = 0$. We can then perform a Taylor expansion in $|\phi| \ll 1$ to arrive at

$$\begin{aligned} \chi(\phi, k) &\approx \left[1 - p_\theta \frac{\phi^2}{2} + iv\phi + O\{\phi^3\} \right]^k \chi(\phi, 0) = \left[1 - \frac{\phi^2}{2} (p_\theta - v^2) + iv\phi + \frac{1}{2} (iv\phi + O\{\phi^{3/2}\})^2 \right]^k \chi(\phi, 0) \\ &\approx \exp \left[-\frac{p_\theta - v^2}{2} k\phi^2 + ivk\phi \right] \chi(\phi, 0) \end{aligned} \quad (\text{B4})$$

Note that we have split the second order term in ϕ for a consistent expansion of the exponential function. As $\chi(\phi, k)$ will be narrowly peaked at small angles ϕ , the corresponding charge distribution will be broad and thus admits a continuous description in n . Assuming an initial pure charge state at n_0 , i.e. $\chi(\phi, 0) = e^{in_0\phi}$, and omitting the periodic boundary conditions, we are left with an approximately Gaussian charge distribution,

$$P(n, k) = \int_{-\pi}^{\pi} \frac{d\phi}{2\pi} \chi(\phi, k) e^{-in\phi} \approx \int_{-\infty}^{\infty} \frac{d\phi}{2\pi} \chi(\phi, t) e^{-in\phi} \stackrel{k \gg 1}{\approx} \frac{1}{\sqrt{2\pi k(p_\theta - v^2)}} \exp \left[-\frac{(n - n_0 - vk)^2}{2k(p_\theta - v^2)} \right] \quad (\text{B5})$$

The normalization has to be corrected manually if the distribution is to be evaluated for discrete n . The mean and the variance of this Gaussian agree with the exact infinite-ladder results in (B2). A mixed initial charge state would result in a mixture of Gaussians, which would eventually converge towards a broader Gaussian.

However, once the charge distribution hits the boundaries in the case of a finite battery, the Gaussian approximations no longer hold and the modified update rule for $P(0, k+1)$ and $P(N, k+1)$ will cause reflections and ultimately lead to a Gibbs-like steady state.

Appendix C: Coherent battery charging

We now consider a battery charged by qubits with energy coherences ($c > 0$). Once again, the time evolution of the battery state has an exact analytic form so long as the charge boundaries are not yet occupied. To this end, we start again from the state transformation rule (A4), from which we see that the impact of the coherences is most prominent at half-swaps, $\theta = \pi/4$. The results presented in the main text were evaluated for half-swaps and $c = 1$, i.e. with qubits prepared in the pure superposition state $|\psi\rangle = \sqrt{q}|g\rangle + \sqrt{1-q}|e\rangle$. In this case, we expect the coherences to cause interference effects as known from quantum random walks. In particular, a battery initialized in an intermediate charge state will evolve into a bimodal charge distribution as the charge steps accumulate, and the two branches of the distribution will simultaneously progress up and down the ladder until they hit the charge boundaries.

The analytic solution to the battery evolution follows after taking the discrete Fourier transform of the density matrix with respect to n, n' , which formally amounts to switching into the periodic phase representation of the infinite-ladder Hilbert space, $\langle \phi | \rho_B | \phi' \rangle := \sum_{n, n'} \langle n | \rho_B | n' \rangle e^{in'\phi' - in\phi} / 2\pi$. Introducing the short-hand notation $\chi(\Phi, \varphi) := \langle \Phi - \varphi/2 | \rho_B | \Phi + \varphi/2 \rangle$, (A4) translates to

$$\begin{aligned} \langle \phi | \rho'_B | \phi' \rangle &= \left\{ 1 - p_\theta + p_\theta \left[(1 - q)e^{i(\phi' - \phi)} + qe^{i(\phi - \phi')} \right] - ic \frac{\Omega}{2} \left[e^{i\alpha} (e^{-i\phi} - e^{-i\phi'}) + e^{-i\alpha} (e^{i\phi} - e^{i\phi'}) \right] \right\} \langle \phi | \rho_B | \phi' \rangle \\ &= \{ 1 - p_\theta [1 - \cos(\phi' - \phi)] + iv \sin(\phi' - \phi) - ic\Omega [\cos(\phi - \alpha) - \cos(\phi' - \alpha)] \} \langle \phi | \rho_B | \phi' \rangle, \\ \Rightarrow \chi'(\Phi, \varphi) &= \left[1 - p_\theta(1 - \cos \varphi) + iv \sin \varphi - 2ic\Omega \sin(\Phi - \alpha) \sin \frac{\varphi}{2} \right] \chi(\Phi, \varphi). \end{aligned} \quad (\text{C1})$$

In this representation, a charge step merely amounts to a multiplicative factor. Notice that, since we employ identically prepared qubits with the same fixed phase angle α , we are free to define the battery phase coordinates ϕ, ϕ' relative to that reference, i.e. set $\alpha = 0$ without loss of generality. The battery state after k charge steps can now be expressed in terms of the initial state as

$$\chi_k(\Phi, \varphi) = \left[1 - p_\theta(1 - \cos \varphi) + iv \sin \varphi - 2ic\Omega \sin \Phi \sin \frac{\varphi}{2} \right]^k \chi_0(\Phi, \varphi). \quad (\text{C2})$$

One can check that the magnitude of the progression factor in square brackets is a number between zero and one, as it should be. It always assumes its maximum at $\varphi = 0$ and decreases at first with growing φ . However, contrary to the incoherent case (B3), the magnitude does not necessarily stay substantially below one for all (Φ, φ) -arguments. Indeed, at $\varphi = \pm\pi$ and $\Phi = \pm\pi/2$, the magnitude reaches up to $\sqrt{1 - 4p_\theta(1 - p_\theta)[1 - 4c^2q(1 - q)]}$, which is unity for coherent qubit superpositions of equal weight ($c = 1, q \approx 1/2$) and half-swaps ($p_\theta = 1/2$). Hence, substantial values of the characteristic function at large angles $|\varphi| \sim \pi$ can persist even after many charge steps, which explains why the charge distribution $P(n, k)$ may exhibit high-frequency interference fringes between neighbouring charge levels; the distribution can be expressed as the Fourier integral

$$P(n, k) = \langle n | \rho_B(k) | n \rangle = \frac{1}{2\pi} \int_{-\pi}^{\pi} d\phi d\phi' e^{in(\phi - \phi')} \chi_k\left(\frac{\phi + \phi'}{2}, \phi' - \phi\right) = \int_{-\pi}^{\pi} \frac{d\Phi}{2\pi} \int_{2|\Phi| - 2\pi}^{2\pi - 2|\Phi|} d\varphi e^{-in\varphi} \chi_k(\Phi, \varphi). \quad (\text{C3})$$

The high-frequency fringes seen in Fig. 2 neither influence the distinct bimodal structure of the charge distribution after $k \gg 1$ nor do they affect the mean and variance appreciably. We shall therefore ignore those high-frequency components and focus on the coarse-grained, quasi-continuous distribution at long times, assuming that the relevant φ -values for the characteristic function are small. Similar to the incoherent case, we can approximate consistently to 2nd order in φ and are left with

$$\chi_k(\Phi, \varphi) \approx \left[1 + i\varphi \underbrace{(v - c\Omega \sin \Phi)}_{=: \gamma(\Phi)} - p_\theta \frac{\varphi^2}{2} + O(\varphi^3) \right]^k \chi_0(\Phi, \varphi) \approx \exp \left[-\frac{p_\theta - \gamma^2(\Phi)}{2} k\varphi^2 + ik\gamma(\Phi)\varphi \right] \chi_0(\Phi, \varphi). \quad (\text{C4})$$

So the characteristic function χ_k approaches a Gaussian shape in φ whose width decreases like $1/\sqrt{k}$, while its complex phase oscillates at a frequency proportional to k ; both depend on the other angle coordinate Φ , as determined by

$$\gamma(\Phi) = v - c\Omega \sin \Phi = (1 - 2q) \sin^2 \theta + c \sqrt{q(1 - q)} \sin 2\theta \sin \Phi. \quad (\text{C5})$$

The charge distribution (C3) can be seen as the $[n - k\gamma(\Phi)]$ -th Fourier component with respect to φ , truncated and averaged over Φ . For large k , the Φ -average will be dominated by the vicinity of the points $\Phi_\pm = \pm\pi/2$ at which the strongly oscillating phase is stationary. Moreover, the width of the Gaussian will be much smaller than π , which allows us to extend the φ -integral in (C3) to infinity. Inserting (C4) and assuming that the battery is initially prepared in a charge eigenstate $|n_0\rangle$ with $\chi_0(\Phi, \varphi) = e^{in_0\varphi}/2\pi$, we get

$$\begin{aligned} P(n, k) &\approx \frac{1}{4\pi^2} \int_{-\pi}^{\pi} d\Phi \int_{-\infty}^{\infty} d\varphi \exp \left\{ -\frac{p_\theta - \gamma^2(\Phi)}{2} k\varphi^2 - i[n - n_0 - k\gamma(\Phi)]\varphi \right\} \\ &= \frac{1}{2\pi} \int_{-\pi}^{\pi} d\Phi \frac{1}{\sqrt{2\pi k[p_\theta - \gamma^2(\Phi)]}} \exp \left\{ -\frac{[n - n_0 - k\gamma(\Phi)]^2}{2k[p_\theta - \gamma^2(\Phi)]} \right\}. \end{aligned} \quad (\text{C6})$$

The result is a smooth average over Gaussians with large widths and displacements. A mixed initial charge state would entail an additional weighted sum over different n_0 , accordingly.

The charge moments are consistently evaluated in the continuum approximation, as we are assuming that the charge distribution (C6) be broad, $\bar{n}^j(k) = \sum_n n^j P(n, k) \approx \int dn n^j P(n, k)$. Specifically, we get

$$\begin{aligned} \bar{n}(k) &\approx n_0 + k \frac{1}{2\pi} \int_{-\pi}^{\pi} d\Phi \gamma(\Phi) = n_0 + vk, \\ \overline{n^2}(k) &\approx \frac{1}{2\pi} \int_{-\pi}^{\pi} d\Phi \left[kp_\theta - k\gamma^2(\Phi) + (k\gamma(\Phi) + n_0)^2 \right] = n_0^2 + k(p_\theta + 2v) + k(k - 1) \left(v^2 + \frac{c^2\Omega^2}{2} \right), \\ \Delta n^2(k) &\approx (p_\theta - v^2)k + \frac{c^2\Omega^2}{2} k(k - 1), \end{aligned} \quad (\text{C7})$$

see also Eq. (9) in the main text. Note that the charge variance only holds for a *pure* initial state, and one must add the initial spread $\Delta n^2(0)$ in the case of a mixture. The average charge moves at the same speed as in the incoherent charging case; there is no difference within the validity bounds of our approximations. The variance, however, gets an additional contribution that grows quadratically with k and thus eventually becomes the dominant cause of charge fluctuations. Indeed, our numerical simulations show that the asymptotic steady state of a coherently charged battery typically yields a flat energy distribution that extends over the whole ladder.

Finally, in order to see that (C6) describes a bimodal distribution, recall that the displacement parameter $\gamma(\Phi)$ in (C5) oscillates between its two extreme values, $\gamma(\Phi_\pm) = v \mp c\Omega$. Since these are stationary points, the Φ -integral will allocate most weight to them and result in distinct maxima around the two respective mean charges $n_\pm \approx n_0 + vk \pm c\Omega k$.

We can make this explicit by performing a stationary phase approximation with respect to Φ in the first line of (C6). Consider two well-behaved real-valued functions $f(x), g(x)$ for $x \in [a, b]$ and let x_n be non-degenerate stationary points well within that interval, at which $f'(x_n) = 0$ and $f''(x_n) \neq 0$. Then

$$\int_a^b dx g(x) e^{ikf(x)} \approx \sum_{x_n} \sqrt{\frac{2\pi i}{k f''(x_n)}} g(x_n) e^{ikf(x_n)} \quad \text{for } k \rightarrow \infty. \quad (\text{C8})$$

Applied to (C6), the approximation is only strictly justified for $|\varphi| \gg 1/k$ and should therefore be taken as a qualitative estimate that may well lead to deviations in the flat parts of the charge distribution while reproducing its more sharply peaked features. We arrive at

$$\begin{aligned} P(n, k) &\approx \frac{1}{4\pi^2} \int_{-\infty}^{\infty} d\varphi \left\{ \sqrt{\frac{2\pi i}{c\Omega k \varphi}} \exp \left[-\frac{p_\theta - \gamma^2(\Phi_+)}{2} k \varphi^2 + ik\gamma(\Phi_+) \varphi \right] + \sqrt{-\frac{2\pi i}{c\Omega k \varphi}} \exp \left[-\frac{p_\theta - \gamma^2(\Phi_-)}{2} k \varphi^2 + ik\gamma(\Phi_-) \varphi \right] \right\} e^{-i(n-n_0)\varphi} \\ &= \frac{Q_+ \left[n - n_0 - k\gamma(\Phi_+), p_\theta - \gamma^2(\Phi_+) \right] + Q_- \left[n - n_0 - k\gamma(\Phi_-), p_\theta - \gamma^2(\Phi_-) \right]}{\sqrt{4c\Omega k}}, \end{aligned} \quad (\text{C9})$$

introducing a distinctively peaked, unnormalized combination of Gaussian distribution and modified Bessel functions,

$$Q_\pm[\mu, \sigma^2] = \frac{1}{\sqrt{4\pi\sigma^2}} e^{-\mu^2/4\sigma^2} \left[\sqrt{|\mu|} I_{-1/4} \left(\frac{\mu^2}{4\sigma^2} \right) \pm \frac{\mu}{\sqrt{|\mu|}} I_{1/4} \left(\frac{\mu^2}{4\sigma^2} \right) \right]. \quad (\text{C10})$$

Although the stationary phase approximation (C9) is noticeably less accurate than the Gaussian approximation (C6), it makes the double-peak structure of the charge distribution around n_\pm explicit.
